PHYSICAL REVIEW B **89**, 121117(R) (2014)

Predicted topological phase transition in the SmS Kondo insulator under pressure

Zhi Li,[1] Jin Li,[1] Peter Blaha,[2] and Nicholas Kioussis[1,*]

[1]*Department of Physics, California State University Northridge, Northridge, California 91330-8268, USA*

[2]*Institute for Materials Chemistry, Vienna University of Technology, A-1060 Vienna, Austria*

(Received 12 November 2013; revised manuscript received 25 February 2014; published 31 March 2014)

Employing density functional calculations we predict that SmS undergoes a topological phase transition from the trivial Kondo insulator (KI) black phase to a topological metallic gold phase under hydrostatic pressure. The underlying mechanism is the pressure-induced change of the $4f$ level from below to above the bottom of the $5d$ conduction band, leading to a d-f band inversion, a parity sign reversal, and the concomitant change of the topological invariant ν_0. This provides a material realization of the topological classification of KIs proposed by Dzero *et al.*

DOI: 10.1103/PhysRevB.89.121117 PACS number(s): 71.27.+a, 03.65.Vf, 62.50.−p, 71.20.Gj

Three-dimensional (3D) topological insulators (TIs), distinguished from ordinary insulators by the $\mathbb{Z}_2$ topological invariant [1–4], are new states of quantum matter which are fully gapped in the bulk of the material but have gapless Dirac fermion states on the surface protected by time-reversal symmetry. Due to the strong spin-orbit coupling (SOC) in these materials, the surface states display an unconventional spin helical texture with the spin direction locked to the two-dimensional electron momentum. Ongoing research efforts focus primarily on the prototypical family of weakly correlated 3D TIs, Bi_2Te_3, Bi_2Se_3, and Sb_2Te_3, where an effective single-electron picture for the electronic structure provides an adequate description.

More recently, the search for novel topological insulator states has extended to the family of correlated TIs, where the interplay between strong electron-electron interactions and the SOC gives rise to topological Mott insulators [5] and topological Kondo insulators (KIs) [6,7]. Dzero *et al.* [6,7] employing the periodic Anderson lattice model developed a topological classification of the emergent bands for KIs, where the topologically nontrivial insulating state depends on the position of re-normalized f level relative to the bottom of the conduction band and the momentum-dependent conduction-f electron hybridization due to the strong SOC interaction on the f sites. The conditions for strong TIs are more likely fulfilled in the mixed valent limit of the Kondo problem, such as in the SmB_6, YbB_{12}, and CeNiSn compounds, containing rare-earth elements with noninteger chemical valence. Subsequent density functional theory (DFT) calculations [8] employing the local density approximation (LDA) + Gutzwiller method predicted that SmB_6 is a strongly correlated TI whose surface states contain three Dirac cones. Recent frequency coding limit cycle and anomalous capacitance [9] experiments and surface conductivity [10,11] measurements have suggested that SmB_6 is a TKI. More recently, density functional theory calculations based on the local density approximation (LDA) and the dynamical mean field theory (DMFT) predicted that the simple cubic PuB_6 [12] is a strongly correlated topological insulator.

Among the strongly correlated KIs, SmS has attracted great interest [13–20] during the past several decades due to its valence and semiconductor-to-metal transition ("black-gold" phase transition) at a relatively low pressure, $p_{B-G} \sim 0.65$ GPa, at room temperature. At ambient pressure SmS is a nonmagnetic semiconductor (black phase) with a small band gap of ∼0.15 eV where the Sm ions have a divalent configuration ($4f^6$) [21,22]. At $p_{B-G} \sim 0.65$ GPa and room temperature it undergoes an isostructural (NaCl-type) first-order phase transition to a metallic phase (gold phase) with a large volume collapse of ∼8% [17,22]. Gold SmS is a homogenous mixed valence state with a Sm valence ranging from 2.6 to 2.8. In the black phase the $4f$ levels, E_{4f}, lie between the valence and $5d$ conduction band split by the crystal field into t_{2g} and e_g subbbands. Upon increasing the pressure the bandwidth of both the $4f$ and $5d$ states increases and at p_{B-G} the $5d$ band overlaps with the $4f$ levels giving rise to a charge transfer from the $4f$ state to the $5d$ conduction band and a concomitant intermediate mixed valence state.

Because of the fluctuating valence and charge transfer between $4f$ and $5d$ orbitals under high pressure [23], the SmS KI offers a unique playground for realizing the trivial-to-nontrivial transition proposed by the tight-binding model calculations of Dzero *et al.* [6]. Furthermore, recent LDA + U calculations for the Pu chalcogenides, which are the actinide counterpart of the Sm chalcogenides (the electronic configuration of the Pu and Sm atoms are $5f^6 6d^0 7s^2$ and $4f^6 5d^0 6s^2$, respectively), have predicted that they are strong TIs at ambient pressure [5]. The rocksalt-structure Pu chalcogenides do not show magnetic order, have anomalous lattice constants, which are too small for both divalent ($5f^6$) and trivalent ($5f^5$) Pu ions, and their room-temperature band gap increases under pressure contrary to conventional knowledge. In contrast, the $4f$ shell in the Sm chalcogenides has smaller radial extension compared to that of the $5f$ shell giving rise to larger $4f$-$4f$ intra-atomic electron interaction, weaker $4f$-$5d$ hybridization which vanishes somewhere in the zone, and narrower $4f$ bands.

In this Rapid Communication, we employ density functional calculations based on the LDA and the modified Becke-Johnson LDA [24] plus Hubbard U (MBJLDA + U) approach to investigate the effects of $4f$ correlation and pressure on the topological nature of SmS. The MBJLDA + U calculations predict that the black phase of SmS is a trivial insulator and undergoes a transition to a nontrivial topological metallic state in the gold phase. This is a material realization of the

*nick.kioussis@csun.edu

topological classification of KIs proposed by Dzero *et al.* [6]. We demonstrate the topological nature by calculating the $\mathbb{Z}_2$ topological invariant which characterizes the global band topology of the occupied Bloch wave functions in the entire Brillouin zone (BZ). This result is further corroborated by the product of the parities for all the occupied states at the time-reversal-invariant momenta (TRIM) points. At ambient pressure inclusion of the intra-atomic Coulomb interaction suppresses the charge transfer between the $4f$ and $5d$ orbitals and renders the band topology of SmS trivial. The underlying mechanism for the topological phase transition is the pressure-induced change of the re-normalized f level relative to the bottom of the $5d$ conduction band due to an increase of the $4f$- and $5d$-derived states bandwidth. This in turn leads to charge transfer between the $4f$ and $5d$ orbitals. This result is further corroborated by the evolution of the band structure and the concomitant $4f$-$5d$ band inversion at the X TRIM points.

The *ab initio* electronic structure calculations employed the all-electron, full-potential linearized augmented plane wave (FPLAPW) method implemented in the WIEN2K code [25]. To better account for the on-site $4f$-electron correlations, we apply the MBJLDA [24] plus U approach that incorporates an on-site Coulomb repulsion U and Hund's rule coupling strength J_H with an approximate correction for self-interaction correction (SIC) [26] for the Sm $4f$ states. We used $R_{\mathrm{MT}} \times K_{\max} = 9.0$, muffin-tin radii of 2.50 a.u. for Sm and 2.30 a.u. for S, respectively, and a $25\times25\times25$ k-point Monkhorst-Pack mesh. We have used the experimental values of 5.97 Å and 5.60 Å for the black and gold phases, respectively. The spin-orbit coupling was included in the self-consistent calculations and the on-site Hund's exchange parameter J_H was set to zero. The basis set consisted of the Sm $4f$, $5d$, $6s$, and $6p$ valence states, the Sm $5s$ and $5p$ states semicore states (treated in a another energy window), and the S $3s$ semicore and $3p$ valence states.

The calculated value of U can depend on theoretical approximations and it may be better to regard the value of U as a parameter and try to specify it from comparison of the calculated physical properties with experiments. The $\mathbb{Z}_2$ is determined by the evolution of the Wannier function center (WFC) in reciprocal space during a "time-reversal pumping" process [27–31]. This corresponds to the phase factor θ of the eigenvalues of the position operator $\hat{\mathbb{X}}$ projected into the occupied subspace. $\mathbb{Z}_2$ is then calculated by the even or odd number of crossings of the evolution of θ with any arbitrary horizontal (θ = const.) reference line, mod 2. For a 3D TI, it is necessary to calculate the invariants, $(\mathbb{Z}_2)_0$ and $(\mathbb{Z}_2)_\pi$, for the two different BZ planes, $k_z = 0$ and $k_z = \pi$. The system is a TI (trivial insulator) if the "strong" topological invariant, $\nu_0 \equiv [(\mathbb{Z}_2)_\pi - (\mathbb{Z}_2)_0]$ (mod 2) is 1 (0). Since SmS has crystal inversion symmetry we have also calculated $\mathbb{Z}_2$ as the product of half of the parity (Kramers pairs have identical parities) numbers, δ_i, for all the occupied states at the TRIM points [32], $(-1)^\nu = \prod_{i=1}^{8} \delta_i$.

Black phase. Figure 1 shows the band structure of SmS calculated with the LDA at the experimental lattice constant of 5.97 Å for the black phase. The calculation reveals that SmS is semimetallic with positive direct energy band, but negative indirect band gap, which is not consistent with the

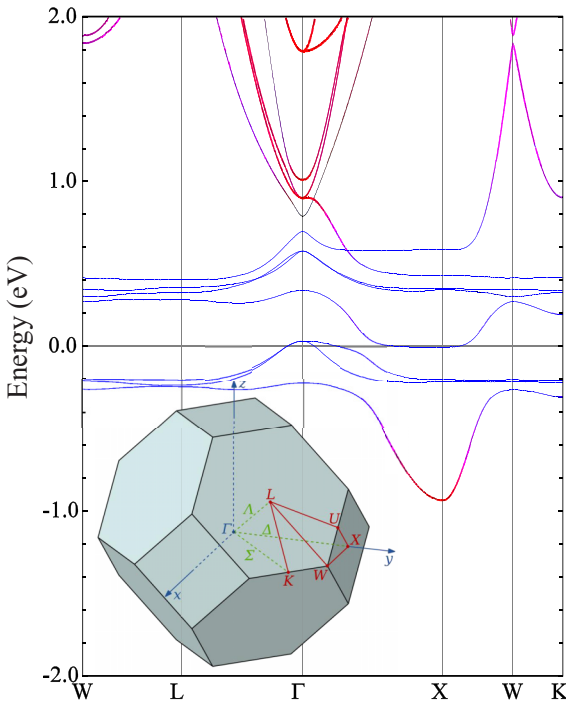

FIG. 1. (Color online) The LDA band structure of the black phase of SmS at ambient pressure at the experimental lattice constant of 5.97 Å. The blue and red colors denote the weight of the Sm $4f$- and $5d$-derived states, respectively. Inset shows the first Brillouin zone and the high-symmetry k points.

experimental results that SmS is a semiconductor with a low band gap of ∼0.15 eV [22]. Each band is twofold degenerate, and the correlated f bands split into occupied $f_{5/2}$-derived bands and unoccupied $f_{7/2}$-derived bands due to the large SOC (∼1.0 eV). The f-derived bands are flat and pinned at the Fermi energy along the W-L direction, but become dispersive along the Γ-X direction, similarly to the band dispersion of the $5f$ states in PuTe [5]. The dispersive electronic bands above the Fermi energy (E_F) are derived mostly from Sm $5d$ states. The bands of primarily $4f$ character are thus placed energetically in between the S $3p$ bands, which are about 4 eV (not shown in Fig. 1) below E_F, and the Sm $5d$ bands. The samarium $4f$ bands hybridize with the $5d$ bands throughout the BZ, except at the TRIM points where the *f*-*d* hybridization vanishes identically, because of the opposite parity of the Sm $4f$- and $5d$-derived states. The weight of the orbital character for the $4f$ and $5d$ states is denoted by blue and red, respectively. Interestingly, the d orbital and f orbital are hybridized into the Γ_7^+ band around the X point.

In analogy with the topological semimetal AuTlTe [33], the topological characterization of the valence energy bands of the semimetallic SmS is still possible due the finite direct band gap throughout the BZ [32]. The band structure of SmS has a *nontrivial* topology because of the band inversion between the $4f$-derived and $5d$-derived states at the X point [$\pi(110)$]. Since the d (f) orbitals are even (odd) under spatial inversion, the product of parities (Table I) of the occupied bands at the three X TRIM points is positive, while that for the other two TRIM points (Γ and four L TRIM points) is negative, similarly

TABLE I. The product of parity eigenvalues for all occupied states at the Γ, three X, and four L TRIM points in the BZ, and the total parity product of all TRIM points, employing the LDA and the MBJLDA + U approaches, respectively. The + and − denote even and odd parity, respectively.

	Γ	3X	4L	Total
LDA (black phase)	−	+ + +	− − − −	−
MBJLDA + U (black phase)	−	− − −	− − − −	+
MBJLDA + U (gold phase)	−	+ + +	− − − −	−

to the case of PuTe. Thus, the LDA method renders SmS a topological semimetal.

We have also carried out calculations employing the MBJLDA [24], which yields accurate band gaps, effective masses, and frontier-band ordering, which are crucial for the correct determination of the TI phase [34]. While the MBJLDA describes accurately the correlation effects of the 5d states, it cannot capture well those of the more localized 4f states, whose treatment still requires a small U value [35,36]. This is similar to the GW + U approach [37], which was also put forward to fix the GW problems for 4f systems. The MBJLDA + U calculations with U of ∼3.0 eV yields a band gap ∼0.20 eV, which is in good agreement with experiment. In Fig. 2(a) we show the band structure of SmS calculated with the MBJLDA + U method at the experimental lattice constant of 5.97 Å for the black phase, in agreement with the fully relativistic Dirac LMTO band structure calculations [15].

As shown schematically in Figs. 3(a) and 3(b) the intra-atomic Coulomb interaction shifts downward the energies of the lower Hubbard band (LHB), which consists of mixed 4$f_{5/2}$ and 4$f_{7/2}$ states, and narrows its bandwidth. The LHB becomes fully occupied and lies in the gap between the the S 3p states and the Sm 5d states. On the other hand, it shifts upward the upper Hubbard band (UHB) which also consists of mixed 4$f_{5/2}$ and 4$f_{7/2}$ states. The UHB is completely unoccupied

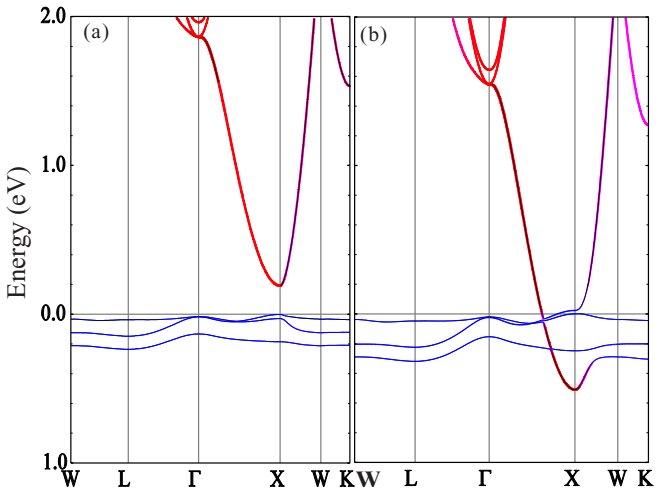

FIG. 2. (Color online) Band structure of SmS with experimental lattice parameter a = 5.97 Å (a) and a = 5.60 Å (b) by MBJLDA + U calculation, with U = 3.0 eV. The weight of 5d and 4f electron is represented by the red and blue color.

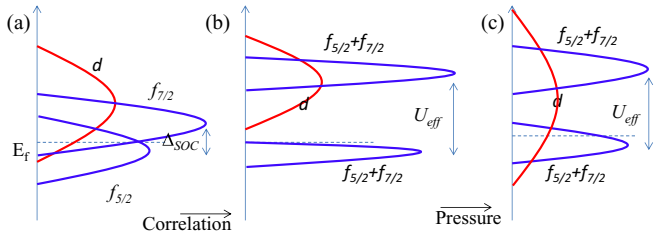

FIG. 3. (Color online) Schematic diagram for the evolution of the density of states of the 5d-derived and the 4f-derived states of SmS (a) in the absence of correlation effects where the SOC splits the f band into the $f_{5/2}$- and $f_{7/2}$-derived states; (b) including the correlation effects which split the f-band into the UHB and LHB by the effective Hubbard U; and (c) increasing the pressure.

and hybridizes with the Sm 5d-derived states. This results in a complete suppression of electron charge transfer between the Sm 4f and 5d states and hence a divalent Sm^{2+} configuration at ambient pressure. The weight of the orbital character for the 4f and 5d states is denoted by blue and red, respectively. The shift of the f band below the 5d band near the X TRIM point leads to a band inversion and hence a parity sign reversal at X (from positive to negative), as listed in Table I, rendering SmS a topological trivial band insulator, consistent with the prediction of Dzero *et al* [6].

Gold phase: Effect of pressure on topological transition. The topological classification of the band structures for KIs [6] invites an intriguing question: Could the pressure-induced change of the 4f level from below to above the bottom of the 5d conduction band lead to a transition from a trivial topological insulator at ambient pressure to a topological metallic state? As shown schematically in Figs. 3(b) and 3(c), the pressure increases the bandwidth of the 5d-derived states and induces a charge transfer between the 4f and 5d orbitals changing in turn SmS in a mixed-valence phase.

Figure 2(b) displays the band structure of SmS calculated with the MBJLDA + U method at the experimental lattice constant of 5.60 Å for the gold phase, where U = 3.0 eV. Comparing Figs. 2(a) and 2(b), it is seen that the fully occupied LHB below E_F in Fig. 2(a) shifts upward and becomes partially occupied while the 5d-derived bands shift downward, and the phase semimetallic, as expected. This leads to a d-f band inversion at the X TRIM point, where as shown in Table I the parity changes from "odd" at ambient pressure to "even" at p_{B-G} ∼ 0.65 GPa, inducing a transition from a trivial topological insulator state to a topological metallic state. Furthermore, as the volume is reduced the 5d and 4f bands become increasingly hybridized, and the d and f bands become broader [also shown schematically in Fig. 3(c)]. The hybridized 4f and 5d bands near the X TRIM point can be be described by an effective low-energy Hamiltonian [6,38] which has two hybridized bands of the form

$$E_{\pm} = \frac{1}{2}\left[\xi_d(\mathbf{k}) + \epsilon_f(\mathbf{k}) \pm \sqrt{[\xi_d(\mathbf{k}) - \epsilon_f(\mathbf{k})]^2 + 4|V_{df}(\mathbf{k})|^2}\right], \quad (1)$$

where $\xi_d(\mathbf{k})$ [$\epsilon_f(\mathbf{k})$] is the bare band dispersion of conduction (localized) 5d (4f) orbital, and $V_{df}(k)$ is the momentum-dependent hybridization between 5d and 4f

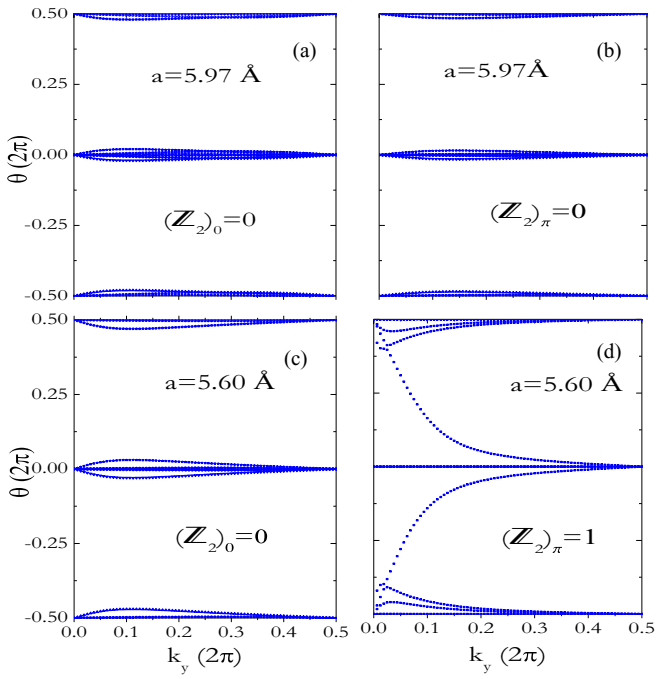

FIG. 4. (Color online) MBJLDA + U calculations of the evolution curves of the Wannier center along k_y in the $k_z = 0$ and $k_z = \pi$ planes in (a) [(c)] and (b) [(d)] for the black (gold) phase, respectively, at the experimental lattice constants. For the black phase $(\mathbb{Z}_2)_0 = (\mathbb{Z}_2)_\pi = 0$ yielding $\nu_0 = 0$, while for the gold phase $(\mathbb{Z}_2)_0 = 0$, $(\mathbb{Z}_2)_\pi = 1$ yielding $\nu_0 = 1$.

states which is odd under spatial inversion and opens up a gap below E_F along the Γ-X symmetry direction, which allows the calculation of Z_2.

In order to corroborate the d-f band inversion and the concomitant sign reversal of the parity at the X TRIM point we have also calculated the $\mathbb{Z}_2$ topological invariant employing the MBJLDA + U method at the experimental lattice constants for the black and gold phases. The evolution curves of the Wannier [29,39,40] centers along the k_y direction in the $k_z = 0$ and $k_z = \pi$ planes are shown in Figs. 4(a) [4(c)] and 4(b) [4(d)] for the black (gold) phase, respectively. For the black phase the evolution curves cross any arbitrary line parallel to the horizontal axis an even number of points for both the $k_z = 0$ and $k_z = \pi$ planes, thus yielding $(\mathbb{Z}_2)_0 = (\mathbb{Z}_2)_\pi = 0$ and $\nu_0 = 0$, confirming that the phase is indeed a trivial topological insulator. In sharp contrast, for the gold phase the evolution curves cross any arbitrary line parallel to the horizontal axis an even (odd) number of points for the $k_z = 0$ ($k_z = \pi$) plane, thus yielding $(\mathbb{Z}_2)_0 = 0$, $(\mathbb{Z}_2)_\pi = 1$, and $\nu_0 = 1$, confirming its topological metallic nature.

In summary, we predict that SmS undergoes a topological phase transition from the trivial Kondo insulator black phase to the topological metallic gold phase under hydrostatic pressure. The underlying mechanism is the pressure-induced change of the $4f$ level from below to above the bottom of the $5d$-derived conduction band due to the increase of the $5d$ bandwidth with decreasing lattice constant. Consequently, the charge transfer between the $4f$ and $5d$ orbitals leads to a d-f band inversion and a parity sign reversal at the X TRIM point, and the concomitant change of the topological invariant ν_0. This provides a material realization of the topological classification of KIs proposed by Dzero *et al.* [6]. The calculations also demonstrate that inclusion of the intra-atomic correlation effects at ambient pressure change the topological nature of the black phase from topological metallic to a topological trivial insulator state.

The research at CSUN was supported by NSF-PREM Grant No. DMR-1205734. J.L. was supported by DTRA Grant No. HDTRA1-10-1-0113.

[1] M. Z. Hasan and C. L. Kane, Rev. Mod. Phys. **82**, 3045 (2010).
[2] Xiao-Liang Qi and Sou-Cheng Zhang, Rev. Mod. Phys. **83**, 1057 (2011).
[3] Yoichi Ando, J. Phys. Soc. Jpn. **82**, 102001 (2013).
[4] J. E. Moore and L. Balents, Phys. Rev. B **75**, 121306(R) (2007).
[5] Xiao Zhang, Haijun Zhang, Jing Wang, Claudia Felser, and Shou-Cheng Zhang, Science **335**, 1464 (2012).
[6] Maxim Dzero, Kai Sun, Victor Galitski, and Piers Coleman, Phys. Rev. Lett. **104**, 106408 (2010).
[7] Maxim Dzero, Kai Sun, Piers Coleman, and Victor Galitski, Phys. Rev. B **85**, 045130 (2012).
[8] Feng Lu, JianZhou Zhao, Hongming Weng, Zhong Fang, and Xi Dai, Phys. Rev. Lett. **110**, 096401 (2013).
[9] D. J. Kim, T. Grant, and Z. Fisk, Phys. Rev. Lett. **109**, 096601 (2012).
[10] D. J. Kim, S. Thomas, T. Grant, J. Botimer, Z. Fisk, and Jing Xia, Nature: Sci. Rep. **3**, 3150 (2013).
[11] Steven Wolgast, Çağlıyan Kurdak, Kai Sun, J. W. Allen, Dae-Jeong Kim, and Zachary Fisk, Phys. Rev. B **88**, 180405(R) (2013).
[12] Xiaoyu Deng, Kristjan Haule, and Gabriel Kotliar, Phys. Rev. Lett. **111**, 176404 (2013).
[13] Z. W. Lu, David J. Singh, and Henry Krakauer, Phys. Rev. B **37**, 10045 (1988).
[14] R. Schumann, M. Richter, L. Steinbeck, and H. Eschrig, Phys. Rev. B **52**, 8801 (1995).
[15] V. N. Antonov, B. N. Harmon, and A. N. Yaresko, Phys. Rev. B **66**, 165208 (2002).
[16] A. Barla, J. P. Sanchez, Y. Haha, G. Lapertot, B. P. Doyle, O. Leupold, R. Rüffer, M. M. Abd-Elmeguid, R. Lengsdorf, and J. Flouquet, Phys. Rev. Lett. **92**, 066401 (2004).
[17] P. P. Deen, D. Braithwaite, N. Kernavanois, L. Paolasini, S. Raymond, A. Barla, G. Lapertot, and J. P. Sanchez, Phys. Rev. B **71**, 245118 (2005).
[18] A. Svane, V. Kanchana, G. Vaitheeswaran, G. Santi, W. M. Temmerman, Z. Szotek, P. Strange, and L. Petit, Phys. Rev. B **71**, 045119 (2005).
[19] E. Annese, A. Barla, C. Dallera, G. Lapertot, J.-P. Sanchez, and G. Vankó, Phys. Rev. B **73**, 140409(R) (2006).

[20] K. Matsubayashi, K. Imura, H. S. Suzuki, S. Ban, G. F. Chen, K. Deguchi, and N. K. Sato, J. Magn. Magn. Mater. **310**, 408 (2007).
[21] P. Misra, *Heavy-Fermion Systems* (Elsevier, Amsterdam, 2008).
[22] C. M. Varma, Rev. Mod. Phys **48**, 219 (1976).
[23] P. Wachter, in *Handbook on the Physics and Chemistry of Rare Earths*, edited by K. A. Gschneider Jr., L. Eyring, G. H. Lander, and G. R. Choppin (Elsevier Science, Amsterdam, 1994), Vol. 19, Chap. 132.
[24] F. Tran and P. Blaha, Phys. Rev. Lett. **102**, 226401 (2009).
[25] P. Blaha and K. Schwarz, Comput. Mater. Sci. **28**, 259 (2003).
[26] V. I. Anisimov, I. V. Solovyev, M. A. Korotin, M. T. Czyzyk, and G. A. Sawatzky, Phys. Rev. B **48**, 16929 (1993).
[27] Liang Fu and C. L. Kane, Phys. Rev. B **74**, 195312 (2006).
[28] Rui Yu, Xiao Liang Qi, Andrei Bernevig, Zhong Fang, and Xi Dai, Phys. Rev. B **84**, 075119 (2011).
[29] Alexey A. Soluyanov and David Vanderbilt, Phys. Rev. B **83**, 035108 (2011).
[30] Lars Winterfeld, Luis A. Agapito, Jin Li, Nicholas Kioussis, Peter Blaha, and Yong P. Chen, Phys. Rev. B **87**, 075143 (2013).
[31] Luis A. Agapito, Nicholas Kioussis, William A. Goddard III, and N. P. Ong, Phys. Rev. Lett. **110**, 176401 (2013).
[32] Liang Fu and C. L. Kane, Phys. Rev. B **76**, 045302 (2007).
[33] Wanxiang Feng, Di Xiao, Jun Ding, and Yuigui Yao, Phys. Rev. Lett. **106**, 016402 (2011).
[34] Yoon-Suk Kim, Martijn Marsman, Georg Kresse, Fabien Tran, and Peter Blaha, Phys. Rev. B **82**, 205212 (2010).
[35] David Koller, Fabien Tran, and Peter Blaha, Phys. Rev. B **83**, 195134 (2011).
[36] Hong Yiang, J. Chem. Phys. **138**, 134115 (2013).
[37] H. Jiang, P. Rinke, and M. Scheffler, Phys. Rev. B **86**, 125115 (2012).
[38] Hiroaki Ikeda and Kazumasa Miyake, J. Phys. Soc. Jpn. **65**, 1769 (1996).
[39] Aarash A. Mostofi, Jonathan R. Yates, Young-Su Lee, Ivo Souza, David Vanderbilt, and Nicola Marzari, Comput. Phys. Commun. **178**, 685 (2008).
[40] Jan Kuně, Ryotaro Arita, Philipp Wissgott, Alessandro Toschi, Hiroaki Ikeda, and Karsten Held, Comput. Phys. Commun. **181**, 1888 (2010).